Chapter 9
A Methodology for Feature Selection and Electrical Capability Prediction of a Coupled Shaker-DUT Model

D. Scheg, J. Heinlen, C. Garcia, L. Redmond, T. Roberts, A. Ramirez, and C. Haynes

Abstract In experimental pre-testing, it is often useful to predict the capability of an electrodynamic shaker to run an environmental test on a given device under test (DUT). In this work, a methodology is proposed for predicting shaker electrical capability through a coupled model and appropriate feature selection using Bayesian classification. The coupled model was formed through a reduced-order finite element model of a DUT and an experimentally-calibrated lumped parameter model of a shaker. A control problem was solved to calculate voltage spectral densities (VSDs) to meet the specified acceleration spectral density (ASD) for the test. Variance was given to model parameters and a Bayesian classifier was employed for feature selection. The Bayesian classifer was verified against three reduced-order model classes and the coupling methodology was validated experimentally. The paper culminates with an example problem which shows that the novel coupling methodology and the Bayesian classifier can be used to predict voltage requirements and select an unknown feature: joint stiffness.

Keywords Environmental testing · Bayesian classification · Reduced-order modeling · Shaker model · Finite element analysis

Introduction

In practice, it is common to run an environmental test on a device under test (DUT). An environmental test is the excitation of a DUT, usually by a shaker, under similar conditions that it would be subjected to in its true application. Often a test operator will not know the dynamic responses of the DUT (mode shapes, modal frequencies, etc.) or know if the shaker has the capability of performing the environmental test due to electrical constraints. Thus, it becomes advantageous to create analytical models for pre-test investigation. Past work investigated modeling a shaker as a lumped parameter system with electrical degrees of freedom (DOFs) to predict shaker requirements in a vibration test [1]. However, this investigation modeled the DUT as mass coupled to the shaker and did not consider the dynamic proper-

D. Scheg
Department of Mechanical Engineering, Purdue University, West Lafayette, IN 47907
e-mail: dscheg@purdue.edu

J. Heinlen
Mathematics & Computer Science Department, Whitworth University, Spokane, WA 992517
e-mail: jheinlen26@my.whitworth.edu

C. Garcia
Department of Mechanical Engineering, New Mexico Institute of Mining and Technology, Socorro, NM 87801
e-mail: chrisgarcia2003@gmail.com

L. Redmond
School of Civil, Environmental Engineering and Earth Sciences, School of Mechanical and Automotive Engineering, Clemson University, Clemson, SC 29634
e-mail: lmredmo@clemson.edu

T. Roberts · A. Ramirez · C. Haynes
Los Alamos National Laboratory, Los Alamos, NM 87545
e-mail: tproberts@lanl.gov; ajrami@lanl.gov; cmhaynes@lanl.gov

Alexandra Karlicek et al. (eds.), *Dynamic Environments Testing, Vol. 7*, Conference Proceedings of the Society for Experimental Mechanics Series, https://doi.org/10.13052/97887-438-0152-8_9

ties of the structure. A high fidelity finite element model (FEM) of the DUT can be used to capture these dynamics in the coupled model. However, a high fidelity FEM tends to have a large computational expense due to the high number of DOFs.

To reduce the computational cost associated with high fidelity models, various reduced-order models (ROM) may be implemented. There are many methods used for creating a ROM such as dynamic mode decomposition [2] and operator inference using deterministic linear regression [3]. In this paper, Guyan reduction (static condensation) [4] and component mode synthesis in the forms of Craig-Bampton and Craig-Chang [5] were used. All three of the used modeling processes begin with static condensation. Craig-Bampton and Craig-Chang also include generalized coordinates to represent a set of eigenmode amplitudes [4]. While both are accurate for static analysis, Craig-Bampton and Craig-Chang are more accurate at high frequency analysis, depending on the included eigenmodes.

ROMs, which retain a fraction of the original DOFs, introduce higher uncertainty, on top of the uncertainty present in the high-fidelity FEM. Specifically, joints have been notoriously difficult to model in the past because the global stiffness of the part is highly influenced by the flexibility of the joints. Past works have investigated the impact of these joints on the dynamics of a system [6–9].

This work proposes a novel methodology to select features, such as the most appropriate ROM or joint stiffness values, of a physically coupled shaker-DUT system, with the goal of determining the voltage needed to run an environmental test. To do so, a shaker model was coupled with a model of the chosen DUT, a box assembly with removable component (BARC). The shaker model was a lumped parameter model [1] and the BARC model was a ROM of a high-fidelity FEM. Given an acceleration specification, such as a benign acceleration spectral density (ASD) that operators are certain the shaker can complete, the voltage required to run the given test of the coupled system was calculated, in the form of voltage spectral density (VSD). The connection between the BARC base and removable component was modeled as sets of springs that were given varied stiffness coefficients. Then, using a Bayesian classifier, the joint stiffness model whose VSD most closely matched the experimental VSD was selected, showing the methodology proposed in this paper can be used to compare modeling techniques for a more accurate representation of a physical system.

Analytical Methods

As aforementioned, the purpose of this project was to: 1. understand the voltage requirements to run an environmental test using a coupled shaker-BARC model, and 2. select features of this system that best represent a set of physical test data. For this purpose, a high DOF model of the BARC system was previously created in Abaqus, a finite element analysis software. This work then implemented ROMs of the BARC to reduce computational expense. The equations of motion (EOMs) from the reduced BARC model and the shaker model were combined to represent the coupled system. The VSD of this coupled EOM was calculated, which estimates the voltage requirements to excite the BARC to the acceleration needed for an environmental test. In order to select features of this system, a Bayesian classifier was used. To demonstrate this method, the spring joint connections between the BARC base and the removable component were varied by using three stiffness coefficients, $k = 100, 1000$, and $10,000\ \mathrm{N/m}$. The Bayesian classifier selected the VSD from the class of stiffness coefficient that was closest to the experimental ground truth VSD.

Reduced-order modeling

The BARC was chosen the DUT because its dynamics are well known. The BARC was modeled in Abaqus using a fine mesh, consisting of over 100,000 DOFs. Three ROM techniques were implemented through Abaqus: Craig-Bampton, Craig-Chang, and Guyan reduction. These reduction methods require the user to specify which DOFs will be retained and fully calculated after reduction. Using engineering judgment, nine nodes were selected that were believed to capture the eight mode shapes of interest. A Modal Assurance Criterion (MAC) was performed, which concluded that the selected nodes adequately retained the overall dynamics of the structure, with an average MAC score of 0.9 for the eight modes. These retained nodes also reflected the positions on the physical BARC where accelerometers would be placed or where the shaker stinger would be connected (see Section 4.2). The first eight natural frequencies of each ROM were compared to the high-fidelity model, of which Craig-Chang had the lowest error. Consequently, this ROM was used for the demonstration of feature selection (joint stiffness) using Bayesian classification.

Joint modeling for classification problem

The joint model was chosen as a mechanism to demonstrate the feasibility of the Bayesian classifier to select appropriate features of a DUT. The joint model consisted of connecting the base of the BARC to the removable component using sets of springs with varying spring stiffness coefficients. Each connection to the base was modeled as four 3-DOF springs, 24-DOF in total. For simplicity of the initial demonstration, all 3 DOFs were assigned the same stiffness in each model class (e.g. the model with $k = 100\mathrm{N/m}$ assigns this stiffness in the x, y, and z direction of the springs).

Shaker model

To solve for the voltage required to excite a system to an acceleration specification, a lumped parameter shaker model was coupled to the FEM of the BARC. The shaker model consists of two mechanical DOFs: the armature and the stinger. It also contains one electrical DOF, the electromotive force, from the resistor and inductor (RL) circuit powering the mechanical components. Altogether, the system's equations of motion are

$$\begin{bmatrix} m_s & 0 & 0 \\ 0 & m_a & 0 \\ 0 & 0 & 0 \end{bmatrix} \begin{Bmatrix} \ddot{x_s} \\ \ddot{x_a} \\ \ddot{i} \end{Bmatrix} + \begin{bmatrix} c_1 & -c_1 & 0 \\ -c_1 & c_1 + c_2 & 0 \\ 0 & -K_f & L \end{bmatrix} \begin{Bmatrix} \dot{x_s} \\ \dot{x_a} \\ \dot{i} \end{Bmatrix} + \begin{bmatrix} k_1 & -k_1 & 0 \\ -k_1 & k_1 + k_2 & K_f \\ 0 & 0 & R \end{bmatrix} \begin{Bmatrix} x_s \\ x_a \\ i \end{Bmatrix} = \begin{Bmatrix} 0 \\ 0 \\ E \end{Bmatrix}. \tag{1}$$

See Table 1 for a complete list of parameters and their values. The electromotive force, E, was controlled to match a given acceleration specification. To calibrate this model, an electromechanical analysis of a the Modal Shop 2060E shaker took place.

These equations were solved using the direct frequency response function (FRF) method at each frequency line. The expression used for this method is

$$-w^2 \begin{bmatrix} m_s & 0 & 0 \\ 0 & m_a & 0 \\ 0 & 0 & 0 \end{bmatrix} + jw \begin{bmatrix} c_1 & -c_1 & 0 \\ -c_1 & c_1 + c_2 & 0 \\ 0 & -K_f & L \end{bmatrix} + \begin{bmatrix} k_1 & -k_1 & 0 \\ -k_1 & k_1 + k_2 & K_f \\ 0 & 0 & R \end{bmatrix} \tag{2}$$

[10],[11]. The mass of the stinger with impedance head attached, m_s, was directly measurable and the mass of the armature, m_a, was found through manufacturing specifications. All other parameters could not be directly measured so they were first estimated then calibrated. The estimation process stems from transfer function simplifications. The equations for these simplifications are as follows:

$$k_1 = (2 \cdot \pi \cdot f_h)^2 \cdot \frac{m_s \cdot m_a}{m_s + m_a}, \tag{3}$$

$$k_2 = (2 \cdot \pi \cdot f_l)^2 \cdot (m_s + m_a), \tag{4}$$

$$K_f = (m_s + m_a) \cdot A_m, \tag{5}$$

$$c_1 = \frac{k_1 \cdot K_f}{(2 \cdot \pi \cdot f_h \cdot (m_s + m_a) \cdot A_h)}, \tag{6}$$

$$c_2 = \frac{2 \cdot \pi \cdot f_l \cdot K_f}{A_l}, \tag{7}$$

where f denotes frequency (Hz) and A denotes the amplitude value at said frequency. The values for amplitude and frequency come from an acceleration over current FRF. The data for this FRF was established through experimental data where the shaker vertically excited the stinger and attached impedance head. Within these two parameters the subscript l denotes a value taken in the lower range of frequency, where the first mode shape can be observed. Similarly the subscript h is used for a value taken at a higher frequency where the second mode shape can be observed. Lastly, the subscript m is used for a value taken in the middle ranges of frequency where there are no modes present. Through analyzing the graphs in Figures 1a, 1b, and 1c, the lower frequency value chosen was 22Hz and the higher frequency value was 3977Hz. The middle frequency value was chosen at 220Hz, a relatively flat part of the FRF graph.

The values found using (3), (4), (5), (6), (7) produced a simplified representation of the system, but ultimately didn't reflect the dynamics of interest. For this reason, each parameter of the system, apart from known values m_s and m_a, was calibrated. This was done by first graphing the experimental data against the not optimized model FRFs: acceleration over current, acceleration over voltage, and impedance. Next, each parameter was optimized using particle swarm optimization or sequential quadratic programming. For each function, upper and lower frequency bounds were set to restrict the optimization to a specific range of the graph, as different frequencies in the FRF functions tended to be affected by the parameters. After the optimization was performed, the calibrated EOM was used as the shaker surrogate in the coupling process. Graphs of each FRF can be seen in Figures 1a, 1b, and 1c.

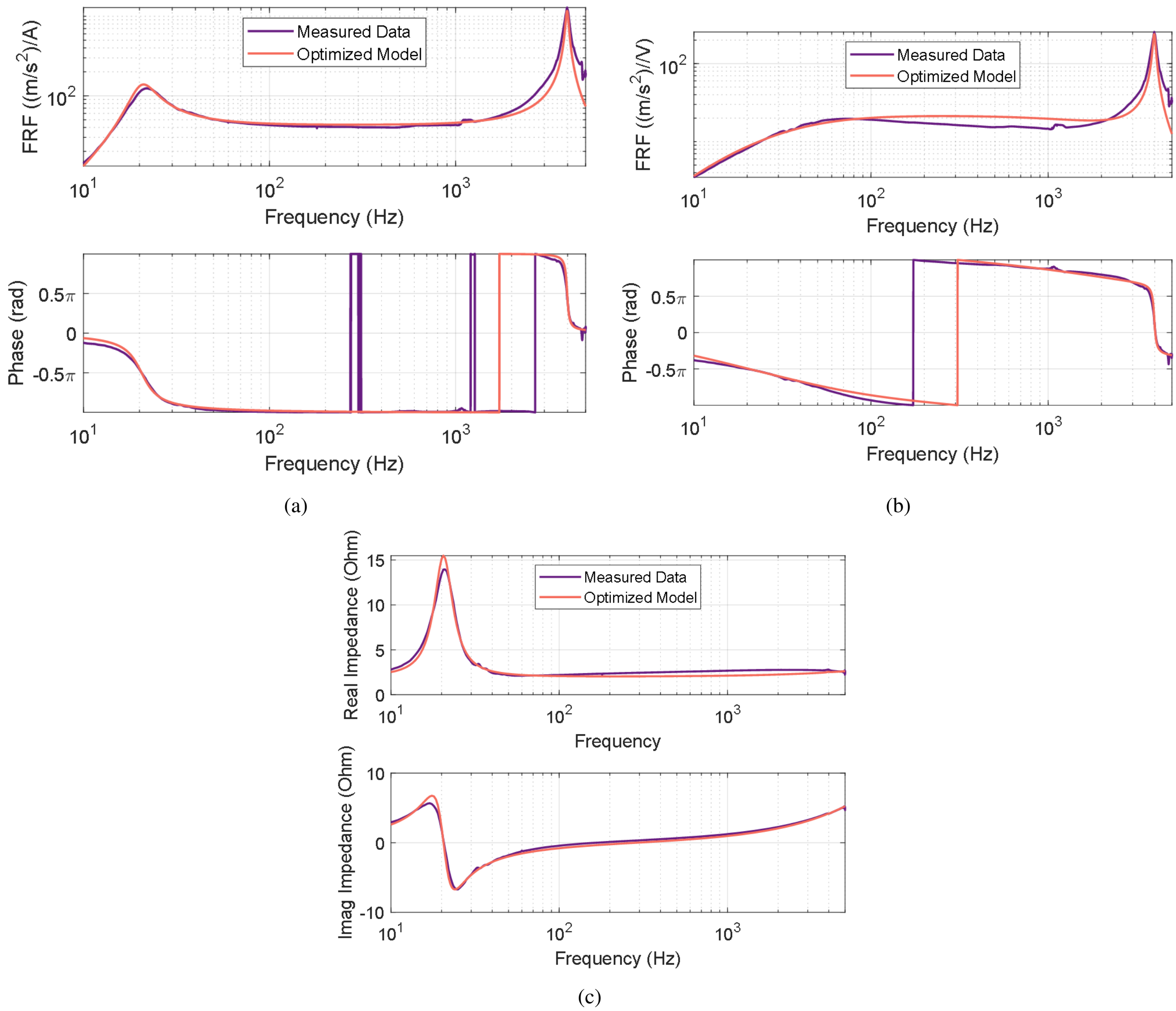

Fig. 1 Shaker model FRFs comparing the measured experimental data and the optimized model for (a) acceleration over current, (b) acceleration over voltage, and (c) impedance.

Coupled system model

In order to model the BARC and the shaker as one coupled system, their mass, damping, and stiffness matrices were first combined into a block diagonal matrix. The upper-left portion of each matrix was from the reduced BARC model and the bottom-right portion was from the calibrated lumped parameter shaker model (3x3). Additionally, in the global stiffness matrix, an arbitrarily high stiffness value, known as k_{glue}, was added at the DOF of excitation to represent the connection between the BARC and stinger. This is the point in the physical system where the shaker's stinger connects to the BARC. This value was also added to the stinger location on the shaker portion of the global matrix and symmetrically, k_{glue}, was subtracted from the off diagonal terms. While the full coupled matrix is to large to show, an example stiffness matrix of the BARC could be written as

$$\begin{bmatrix} k_{11} & k_{12} & k_{13} \\ k_{21} & k_{22} & k_{23} \\ k_{31} & k_{32} & k_{33} \end{bmatrix}. \tag{8}$$

Coupling the example matrix 8 with the stiffness matrix from equation 1 at DOF 3 gives the example coupled matrix of

$$\begin{bmatrix} k_{11} & k_{12} & k_{13} & 0 & 0 & 0 \\ k_{21} & k_{22} & k_{23} & 0 & 0 & 0 \\ k_{31} & k_{32} & k_{33}+k_{glue} & -k_{glue} & 0 & 0 \\ 0 & 0 & -k_{glue} & k_1+k_{glue} & -k_1 & 0 \\ 0 & 0 & 0 & -k_1 & k_1+k_2 & K_f \\ 0 & 0 & 0 & 0 & 0 & R \end{bmatrix}. \tag{9}$$

Because the overarching goal of this project was to model a shaker's ability to run an environmental test with a given DUT, a flat ASD of 0.0125 $(\mathrm{m/s^2})^2/\mathrm{Hz}$ was controlled at a specified point on the BARC, on both the physical and modeled BARC. The specified point was the retained node (see Section 3.1) on the removable component of the BARC. The FRFs from this data were calculated using methods described above (see Section 3.3), and were algebraically manipulated to solve for the electromotive force, resulting in VSD: power spectral density ($\mathrm{V^2/Hz}$) as a function of frequency (Hz). VSD is the form of data that was used to compare classes within the Bayesian classifier. Additionally, the coupled system model was validated against the experimental ground truth by comparing their VSDs and showing they qualitatively matched (see section 4 and Figure 5).

Bayesian classification methodology

Bayesian classification theory

A Naïve Bayesian classifier works by classifying an object X as class C when the posterior probability is highest, that is, when $P(C_i|X)$ for $i = 1, ..., m$ is maximum. Bayes' Theorem shows that

$$P(C_i|X) = \frac{P(X|C_i)P(C_i)}{P(X)}. \tag{10}$$

$P(X)$, the probability that X is the observation chosen, is constant in equation 10. All classes are assumed to be equally likely, that is, $P(C_1) = P(C_2) = ... = P(C_m)$ - a valid assumption since a constant number of observations was used from each class. Therefore, in equation 10, the only non-constant value to be maximized on the right-hand side is $P(X|C_i)$ [12].

In Naïve Bayesian Classification, it is assumed that all m points in each observation are independent of each other. The densities of each class's multivariate normal distribution were calculated under this assumption. These densities were normalized by dividing each class by the total density of all classes, resulting in the probability that the observation came from class C, or $P(X|C_i)$. The class with the maximum probability/density for the observation was selected as the best class.

Application of bayesian classification

As mentioned above, this project used Bayesian classification to select features of a shaker-DUT model that most closely matched the physical system, with the goal of determining if a shaker is adequate for an experimental test. As voltage was one of the limiting factors of a shaker test, VSDs were chosen as the medium to compare models. That is, the Bayesian classifier would select the class of model whose VSDs most closely matched the ground truth VSD. As an initial verification, coupled systems using three different ROMs of the BARC were compared to a sampled VSD coming from the VSD distribution of the shaker-DUT model using Craig-Chang for the ROM. Once the classifier was verified to correctly choose the Craig-Chang representation of the BARC, three joint model stiffnesses were compared to the experimental VSD.

As mentioned previously, the classifier needs to know the distribution of VSDs from each class of shaker-DUT model being compared in order to determine the probability the physical data comes from each model class's VSD distribution. There was uncertainty in the shaker parameters as well as the BARC model, so these parameters were each assigned a normal distribution according to the uncertainty of the parameter. In Table 1, there is a list of these varied parameters, as well as the mean and variance of the normal distribution they were selected from. Mean was determined by the measured/optimized values, and standard deviation was 10% of the mean value. For each shaker-DUT model class, Latin hypercube sampling was used to sample from all parameter distributions and calculate the VSD resulting from each sampled set of parameters. Note that the parameters were varied from the same distributions shown in Table 1 for every model class.

The resulting coupled system VSDs for each class maintained a multivariate normal distribution. The VSD distributions for each ROM are shown in Figure 2. It was also found that classifying with only the frequencies corresponding to the first eight minima of the VSD, which usually correspond to the natural frequencies, was sufficient for distinction in classification.

Table 1 Parameter mean and standard deviation in the shaker and BARC model. Mean values were determined by the results of parameter optimization or measurement. Standard deviations were set to be 10% of the mean value. Stinger mass, armature mass, and resistance were determined not to have a significant amount of uncertainty, so they were not varied.

Parameter (units)	Symbol	Mean	Standard Deviation
Stinger mass (kg)	m_s	0.0252	0
Armature mass (kg)	m_a	0.2700	0
Stinger damping coefficient $(\mathrm{Ns/m})$	c_1	21.1654	2.1165
Flexure damping coefficient $(\mathrm{Ns/m})$	c_2	11.9088	1.1909
Stinger stiffness $(\mathrm{N/m})$	k_1	$1.4392 \cdot 10^7$	$1.4392 \cdot 10^6$
Flexure stiffness $(\mathrm{N/m})$	k_2	$4.9129 \cdot 10^3$	491.2915
Coupling coefficient	K_f	12.6722	1.2672
Resistance (Ω)	R	2	0
Inductance, real (H)	$Re(L)$	$9.0000 \cdot 10^{-5}$	$9.0000 \cdot 10^{-6}$
Inductance, imaginary (H)	$Im(L)$	$-9.0000 \cdot 10^{-7}i$	$9.0000 \cdot 10^{-8}i$
Young's Modulus (Pa)	E	$69 \cdot 10^9$	$69 \cdot 10^8$

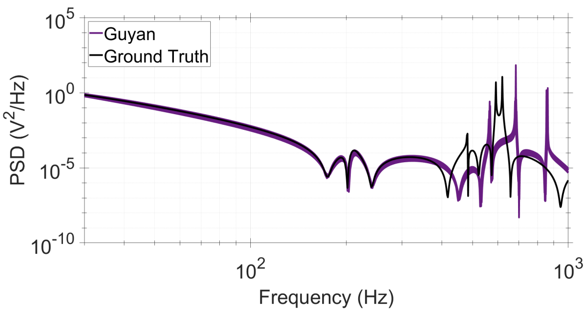

(a)

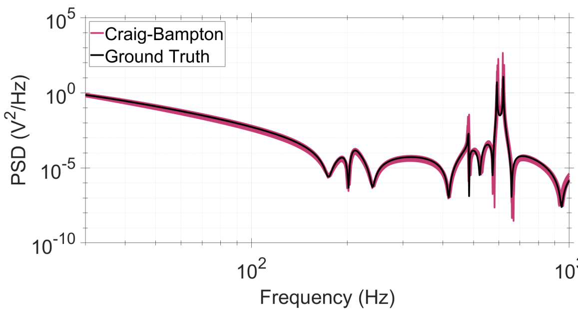

(b)

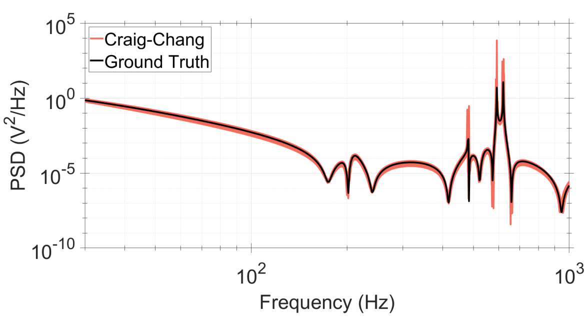

(c)

Fig. 2 VSD outputs of the three ROMs plotted against a Craig-Chang sampled ground truth. Ten outputs for each class are shown, however 75 were as (a) Guyan reduction (b) Craig-Bampton reduction (c) Craig-Chang reduction.

The magnitude of the VSD was not used for classification. Figure 3 is an example of points that were selected for classification in ten iterations of the VSDs generated using Guyan reduction. Note that although the 2-D graph is shown, only the frequency values were used for classification.

Initial verification of bayesian classification for coupled system selection

For initial verification, three reduced-order modeling methods were compared: Guyan reduction, Craig-Chang, and Craig-Bampton (see Section 3.1). For ground truth, a VSD from the Craig-Chang distribution was sampled (see Figure 2). The results of the Bayesian classifier can be seen in Table 2. The Craig-Chang ROM had, by far, the closest match to the sampled ground truth. This validated that the classifier could distinguish between VSDs of different classes and accurately make

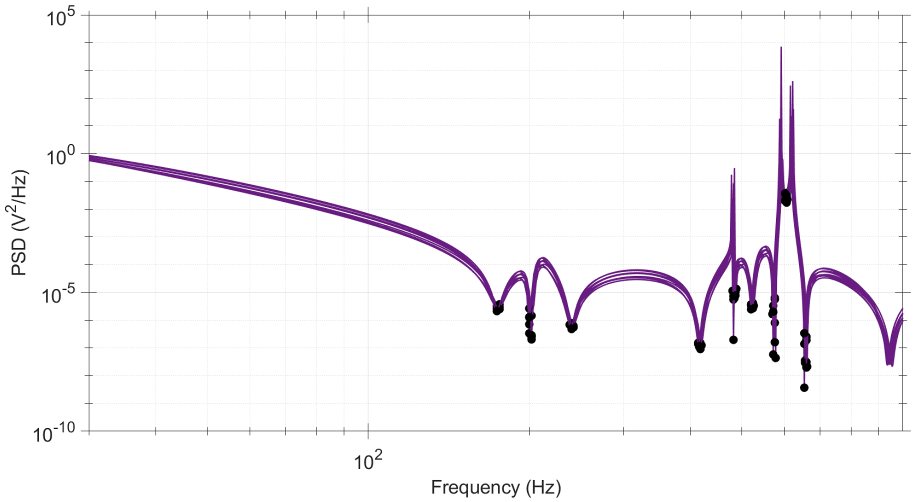

Fig. 3 A sample of VSDs from the normal distribution of VSDs calculated using Guyan reduction. The first eight local minima in the VSD were used for classification, and are highlighted as black dots.

predictions. After verification, the three joint stiffness values were compared and ground truth was determined experimentally, shown in Sections 4 and 5.

Table 2 Normalized and unnormalized probabilities output from the Bayesian classifier performed for verification on the three ROMs.

Class	Unnormalized Bayes' Prediction	Normalized Bayes' Prediction
Guyan Reduction	$e^{-24651.66}$	0
Craig-Bampton CMS	$e^{-39.13302}$	0
Craig-Chang CMS	$\boldsymbol{e^{-9.58068}}$	**1**

Experimental Methods

Shaker setup

Before coupling the shaker and BARC models (see Section 3.4), the shaker model was calibrated using experimental data. To do this, a stinger and impedance head were attached to the physical shaker and a broadband frequency from 5Hz to 6000Hz was provided, which was found to be adequate to detect both mode shapes. The first mode occurs when the armature and stinger are moving in phase, and the second mode occurs when the armature and stinger are moving out of phase. During the experimental test, voltage, current, and displacement were measured. Consequently, three FRFs were calculated as described in Section 3.3 and as seen in Figures 1a, 1b, and 1c.

BARC setup

To obtain the physical data used for the feature selection demonstration, the BARC was bolted to the shaker's stinger and was hung using fishing wire and rubber bands to imitate free-free boundary conditions (see Figure 4). The stinger of the shaker was bolted to the BARC at a point corresponding to a retained node in the ROMs (see Section 3.1). Similarly, accelerometers were attached at points also corresponding to retained nodes, including the chosen control point on the removable component of the BARC. The BARC was excited with a frequency range of 30 Hz to 1000 Hz, and Siemens Testlab was used to control to the specified ASD at the control point (see Section 3.4). Then, the VSD was computed and is used as the ground truth to compare against the VSDs of the modeled system.

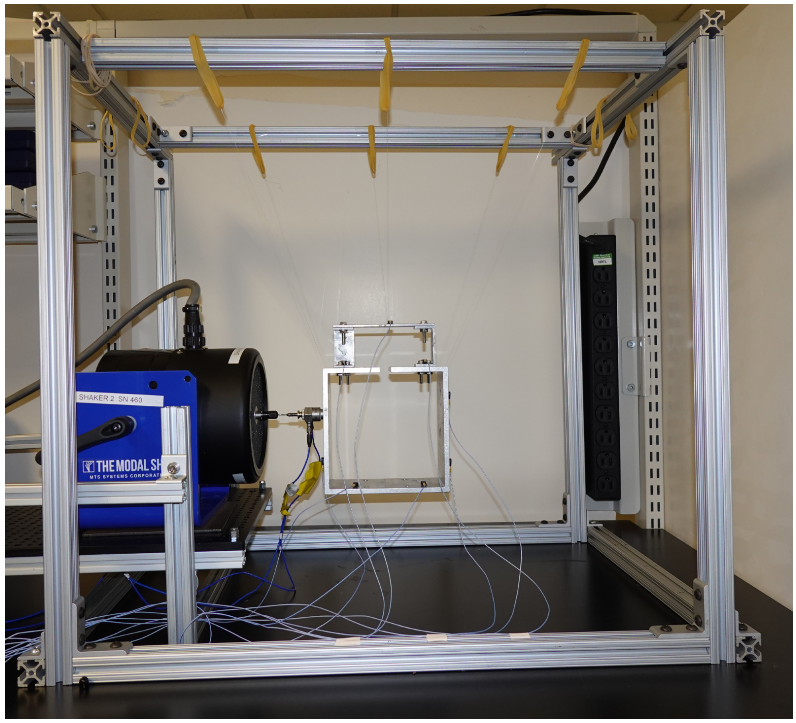

Fig. 4 The experimental set up with the BARC attached to the shaker in free-free boundary conditions.

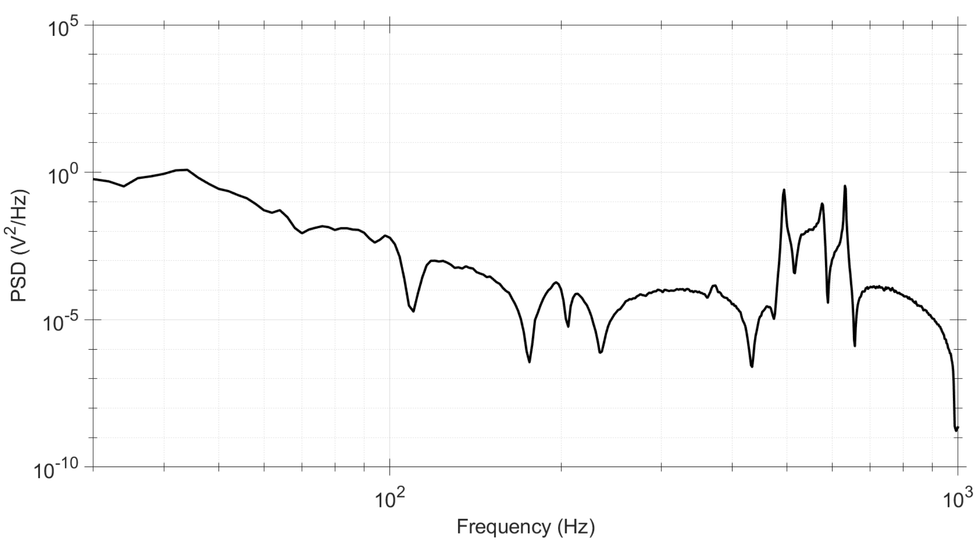

Fig. 5 The VSD from experimental data and used as ground truth in classification.

Analysis

After the coupled system was validated against the experimental ground truth and the Bayesian classifier was shown to distinguish VSDs of different ROMs (see Section 3.5.3), focus was turned to feature selection of the coupled model. Specifically, three values of joint stiffness between the base of the BARC and the removable component were compared: $k = 100, 1000$, and $10,000$ $(\mathrm{N/m})$ as shown in Section 3.2. 75 iterations were generated for each of the three classes, adding synthetic noise from a normal distribution to each iteration. The VSDs were then calculated and Figure 6 shows 10 representative iterations of each class plotted against the experimental ground truth.

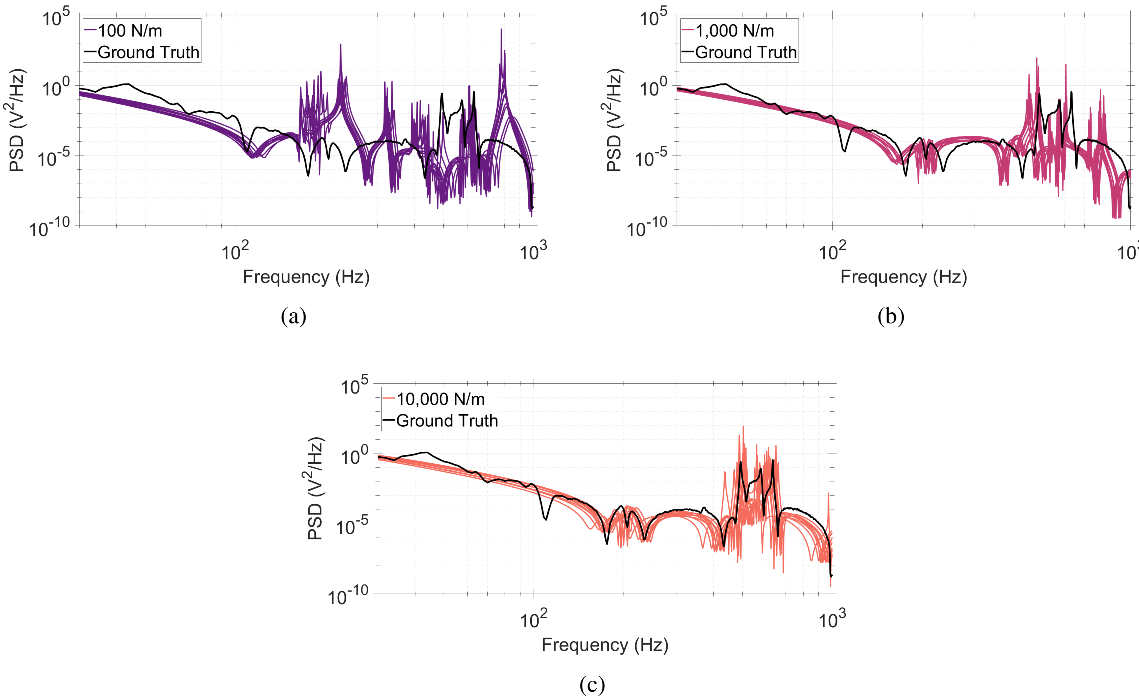

Fig. 6 VSD outputs of the three different spring stiffness coefficients plotted against the experimental ground truth. (a) Stiffness of 100 $\mathrm{N/m}$ (b) Stiffness of 1000 $\mathrm{N/m}$ (c) Stiffness of 10000 $\mathrm{N/m}$.

The model failed to pick up the resonance that is occurring at $\sim$140 Hz and some of the oscillatory behaviors of the voltage quantity in the experimental ground truth. This is most likely a byproduct of the simplifications that were made in the lumped parameter model of the shaker, the simplification of the joint stiffness as being identical in all 3 directions, and also uncertainty in the Abaqus model of the BARC. The uncertainty in the FEM model of the BARC comes from the reduced order methods, indicated by the MAC diagonal values not being correlated to a value of one. However, qualitatively, this verifies a few components of the model. Firstly, the two systems, the Abaqus mass and stiffness and the lumped parameter model, are being coupled correctly. Secondly, the lumped parameter model that was calibrated using experimental data is sufficient to pick up the dynamic responses of the experimental system. Lastly, at higher stiffness values of the joint connections the Abaqus model of the BARC is tracking the dynamic responses of the experimental setup adequately. Interestingly, when visually inspecting the system at the fundamental frequency in Abaqus with a 100 $\mathrm{N/m}$ stiffness value given for the springs, the top removable component separated from the box assembly base. This is most likely why there is less of a correlation to the ground truth in Figure 6a in comparison to the higher stiffness classes in Figures 6b and 6c.

These distributions were then imported into the Bayes' classifier and the minima were used to predict which of the three models best matched the ground truth. The classifier results shown in Table 3 predicted that the 10,000 $\mathrm{N/m}$ stiffness class most closely matched the experimental ground truth. The normalized probability of 1 shows that the joint connection of the physical system is best represented by a high stiffness value.

Table 3 Normalized and unnormalized probabilities output from the Bayesian classifier performed on three spring stiffness values.

Class	Unnormalized Bayes' Prediction	Normalized Bayes' Prediction
K value = 100	$e^{-488385.36}$	0
K value = 1,000	$e^{-3117.868}$	0
K value = 10,000	$\boldsymbol{e^{-488.1526}}$	**1**

Conclusion

Coupling a shaker model with a ROM of a DUT allows a user to asses the shaker's voltage capability to run an environmental test. Not only can this tool be used to inform a user's choice of shaker, but also to ensure that the structural dynamics of the DUT will be accurately measured during the environmental test. In addition, a Bayesian classifier can be used to select features, such as spring stiffness, of the DUT model that best represent the physical system. In a future work, this tool may be used to compare and select other model features, such as joint modeling techniques. Additionally, future work could explore limiting facets of a shaker other than voltage, such as force.

Acknowledgments We would like to gratefully acknowledge: Shashir Sharma for assisting with the Bayesian classifier, Stephen Wright for lending a Python to Abaqus wrapper, and Sean Kelly and Shannon Danforth for the help with reduced-order modeling.
This research was funded by Los Alamos National Laboratory (LANL) through the Engineering Institute's Los Alamos Dynamics Summer School. The Engineering Institute is a research and education collaboration between LANL and the University of California, San Diego's Jacobs School of Engineering. This collaboration seeks to promote multidisciplinary engineering research that develops and integrates advanced predictive modeling, novel sensing systems, and new developments in information technology to address LANL mission relevant problems.

References

1. Schultz, R. "Calibration of shaker electro-mechanical models". In Special Topics in Structural Dynamics & Experimental Techniques, Volume 5: Proceedings of the 38th IMAC, A Conference and Exposition on Structural Dynamics 2020, pages 133-144. Springer (2021)
2. Huhn, Q.A., Tano, M.E., Ragusa, J.C., and Choi, Y. "Parametric dynamic mode decomposition for reduced order modeling". Journal of Computational Physics, 475:111852 (2023)
3. McQuarrie, S.A., Guo, M., and Willcox, K. "Bayesian operator inference for data-driven reduced-order modeling". In 2022 Fall Western Sectional Meeting. AMS.
4. Flodén, O., Persson, K., and Sandberg, G. "Reduction methods for the dynamic analysis of substructure models of lightweight building structures". Computers & Structures, 138:49-61 (2014)
5. MORE, M. "Craig-bampton method" (2000)
6. Langer, P., Sepahvand, K., Guist, C., and Marburg, S. "Finite element modeling for structural dynamic analysis of bolted joints under uncertainty". Procedia engineering, 199:954-959 (2017)
7. Ma, X., Bergman, L., and Vakakis, A. "Identification of bolted joints through laser vibrometry". Journal of Sound and Vibration, 246(3):441-460 (2001)
8. Reid, J.D. and Hiser, N.R. "Detailed modeling of bolted joints with slippage". Finite elements in analysis and design, 41(6):547-562 (2005)
9. Ibrahim, R.A. and Pettit, C. "Uncertainties and dynamic problems of bolted joints and other fasteners". Journal of sound and Vibration, 279(3-5):857-936 (2005)
10. "Section 24: Frequency response analysis". https://help.autodesk.com/view/NINCAD/2022/ENU/?guid=GUID-FCA4E4B5-1A53-480E-A43A-A208E8F3C97E (2024) [Online; accessed 2024-09-25].
11. Kabe, A.M. and Sako, B.H. "Chapter 6 - experimental structural dynamics". In Kabe, A.M. and Sako, B.H., editors, Structural Dynamics Fundamentals and Advanced Applications, pages 429-511. Academic Press (2020)
12. Han, J., Kamber, M., and Pei, J. "8 - classification: Basic concepts". In Han, J., Kamber, M., and Pei, J., editors, Data Mining (Third Edition), The Morgan Kaufmann Series in Data Management Systems, pages 327-391. Morgan Kaufmann, Boston, third edition edition (2012)